

## INFLUENCE OF PARTICLE SIZE ON THE CRYSTALLIZATION PROCESS AND THE BIOACTIVE BEHAVIOR OF A BIOACTIVE GLASS SYSTEM

X. Chatzistavrou<sup>1</sup>, T. Zorba<sup>1</sup>, K. Chrissafis<sup>1</sup>, G. Kaimakamis<sup>1</sup>, E. Kontonasaki<sup>2</sup>, P. Koidis<sup>2</sup> and K. M. Paraskevopoulos<sup>1\*</sup>

<sup>1</sup>Solid State Physics Section, Physics Department, Aristotle University of Thessaloniki, 54124 Thessaloniki, Greece

<sup>2</sup>School of Dentistry, Department of Fixed Prosthesis and Implant Prosthodontics, Aristotle University of Thessaloniki 54124 Thessaloniki, Greece

Bioactive glasses have attracted considerable interest in recent years, due to their technological application, especially in biomaterials research. Differential scanning calorimetry (DSC) has been used in the study of the crystallization mechanism in the  $\text{SiO}_2\text{--Na}_2\text{O--CaO--P}_2\text{O}_5$  glass system, as a function of particle size. The curve of the bulk glass presents a slightly asymmetric crystallization peak that could be deconvoluted into two separate peaks, their separation being followed in the form of powder glasses. Also, a shift of the crystallization peaks to lower temperatures was observed with the decrease of the particle size. FTIR studies – that are confirmed by XRD measurements – proved that the different peaks could be attributed to different crystallization mechanisms. Moreover, it is presented the bioactive behavior of the specific glass as a function of particle size. The study of bioactivity is performed through the process of its immersion in simulated human blood plasma (simulated body fluid, SBF) and the subsequent examination of the development of carbonate-containing hydroxyapatite layer on the surface of the particles. The bioactive response is improved with the increase of the particle size of powders up to 80  $\mu\text{m}$  and remains almost unchanged for further increase, following the specific surface to volume ratio decrease.

**Keywords:** bioactive glass, crystallization, DSC, FTIR, particle size, SBF

### Introduction

Bioactive glasses have numerous applications in the repair and reconstruction of diseased and damaged tissues. The possibility of controlling a range of their chemical properties and the rate of bonding to tissues, differentiate them from other bioactive ceramics and glass-ceramics. The most reactive glass compositions develop a stable, bonded interface with soft tissues. The primary advantage of bioactive glasses is their rapid rate of surface reaction which leads to fast tissue bonding. Their main disadvantage is its mechanical weakness and low fracture toughness due to an amorphous two-dimensional glass network, which make them unsuitable for load-bearing applications [1].

In most of applications, bioactive glasses are used in form of powders – with certain particle size- producing coatings on different substrates, which are incurred at various heat treatments [2, 3]. Different conditions of thermal treatments of bioactive glass powder can affect subsequent crystallization processes and thus may influence its bioactivity and cellular reactions. Moreover, it is observed that apart from different heat treatments, the crystallization mechanism is dependent on particle size of powders [4].

In the investigation of crystallization and nucleation in a glass, it is important to acquire information about the temperature range at which nucleation and growth reactions take place, thus making it possible to control the microstructure of the glass formed through a scheduled heat treatment. DSC is a rather simple method to obtain useful quantitative information about nucleation and crystallization mechanisms in glass forming systems [5, 6].

The object of this investigation was the study of the mechanism of crystallization in the  $\text{SiO}_2\text{--Na}_2\text{O--CaO--P}_2\text{O}_5$  bioactive glass system as a function of particle size. Furthermore, the bioactive behavior dependence of the specific glass system on particle size is studied, through the process of immersion in SBF and the examination of the developed hydroxylcarbonate apatite (HCA) layer on the surface of the particles.

### Experimental

#### Materials and methods

High-purity silica and reagent-grade calcium, sodium carbonate, and calcium phosphate were weighed and mixed to obtain bioactive glass in the system

\* Author for correspondence: kpar@auth.gr

SiO<sub>2</sub>–Na<sub>2</sub>O–CaO–P<sub>2</sub>O<sub>5</sub> (45SiO<sub>2</sub>, 24.5Na<sub>2</sub>O, 24.5CaO, 6.0P<sub>2</sub>O<sub>5</sub> in mass%). The glass was melt in a Pt crucible at 1450°C in a high temperature furnace, where it was kept for 4 h to ensure that the melt was homogeneous and bubble free, and then, the melt was poured and quenched in water. The formation of the bioactive glass – in the specific system – was confirmed by FTIR analysis and scanning electron microscopy with associated energy dispersive spectroscopic analysis (SEM-EDS). The quenched glass was ground and screened – by a system of multiple sieving – to five different regions of particle size: less than 20, 20–40, 40–80 and 80–140 μm and bulk.

The thermal behaviour of bioactive glass in the bulk form and in the form of powdered samples of different grain size ranges was studied using differential thermal and thermogravimetric analysis (DTA/TG). Thermal analysis was performed with a Setaram thermogravimetric-differential thermal analyzer SETSYS 16/18 TG-DTA (1750°C rod), under the conditions of heating rate 10°C min<sup>-1</sup>, up to 1400°C – in argon atmosphere –, and furnace cooling. The mass in all studied samples was about 40 mg.

In order to follow the bioactivity evolution, samples with different particle size and the same mass ( $m=40$  mg) were soaked for the same time period (1 day and 2 days) in a solution that simulates human blood fluid (SBF) [7, 8], with a composition that can be found in Table 1. SBF was prepared by dissolving appropriate quantities of reagent grade chemicals of NaCl, NaHCO<sub>3</sub>, KCl, K<sub>2</sub>HPO<sub>4</sub>·3H<sub>2</sub>O, MgCl<sub>2</sub>·6H<sub>2</sub>O and CaCl<sub>2</sub> in distilled water, as described by Kokubo *et al.* [7] and the ion concentrations were confirmed using atomic absorption spectroscopy (AAS). The pH of the solution was buffered at 7.25 with tris(hydroxymethyl)amine-methane and hydrochloric acid at 37°C.

In order to attend the time dependence of the apatite layer formation with the particle size, the powders were immersed in SBF solutions with a specific volume of immersion liquid – the same for all samples – and were stored in an incubator at 37°C. After one and two days of immersion, powder samples were filtrated, rinsed with distilled water and air-dried. Then, the same quantity from each powder with different particle sizes ( $m\sim 1.5$  mg), was mixed with KBr and was pressed in a vacuum press, in order to be produced pellets with 13 mm diameter and 0.6% conciseness, which were examined with FTIR.

FTIR measurements were carried out with a Bruker spectrometer IFS 113v and the spectra were

collected in the transmittance mode, in MIR region (5000–400 cm<sup>-1</sup>). Due of the increase of noise in spectra with the increase of the particle size of the powders, for each spectrum 128 consecutive scans were recorded with a resolution 2 cm<sup>-1</sup>, thus the transmittance bands of CO<sub>3</sub><sup>2-</sup> at the spectra are observed.

## Results and discussion

### *Crystallization process dependence on particle size*

In Fig. 1 is presented the DSC curve obtained from a powdered sample of the bioactive glass system SiO<sub>2</sub>–Na<sub>2</sub>O–CaO–P<sub>2</sub>O<sub>5</sub> with particle size less than 20 μm. There are four characteristic features: the glass transition ( $T_g$ ) at 555°C, two exothermic crystallization peaks ( $T_{c1}$  and  $T_{c2}$ ) at 700 and 795°C respectively, and the melting process that takes place in the range 1100–1250°C.

The TG analysis, confirms that at lower temperatures (<200°C) there is a small reduction in mass about 0.08%, that is attributed to the evaporation of water which was included in bioactive glass mass during the preparation process, and at higher temperatures the mass remains unchanged.

In the corresponding curves (Fig. 2) in the region of crystallization of all powdered samples we follow the presence of two discrete crystallization peaks and their behavior seems to be dependent on the particle size. Decreasing the particle size the first peak become sharper and for powders with particle size <80 μm the two peaks are clearly separated. However, increasing the particle size, the first peak – at

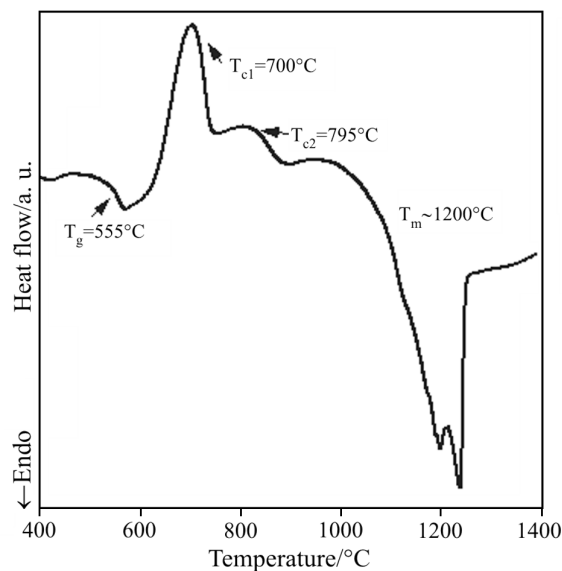


**Fig. 1** DSC curve of powdered bioactive glass in system SiO<sub>2</sub>–Na<sub>2</sub>O–CaO–P<sub>2</sub>O<sub>5</sub> (particle size <20 μm) at heating rate of 10°C min<sup>-1</sup> (heat flow)

**Table 1** Ion concentrations of the simulated body fluid (mmol dm<sup>-3</sup>)

Na <sup>+</sup>	K <sup>+</sup>	Mg <sup>2+</sup>	Ca <sup>2+</sup>	Cl <sup>-</sup>	HCO <sub>3</sub> <sup>-</sup>	HPO <sub>4</sub> <sup>2-</sup>
142.0	5.0	1.5	2.5	147.8	4.2	1.0

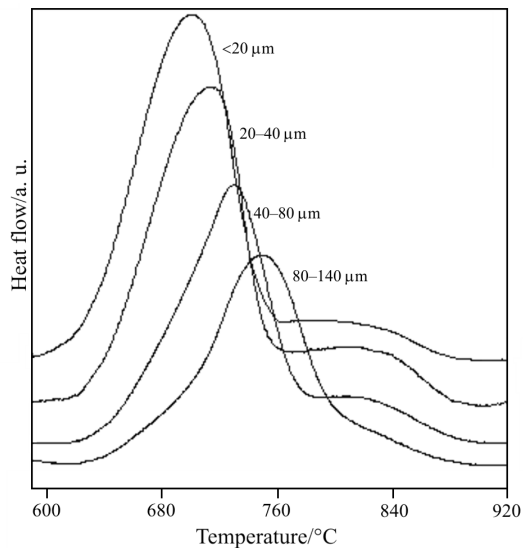


**Fig. 2** DSC curves of bioactive glass powder as a function of particle size (heating rate  $10^{\circ}\text{C min}^{-1}$ )

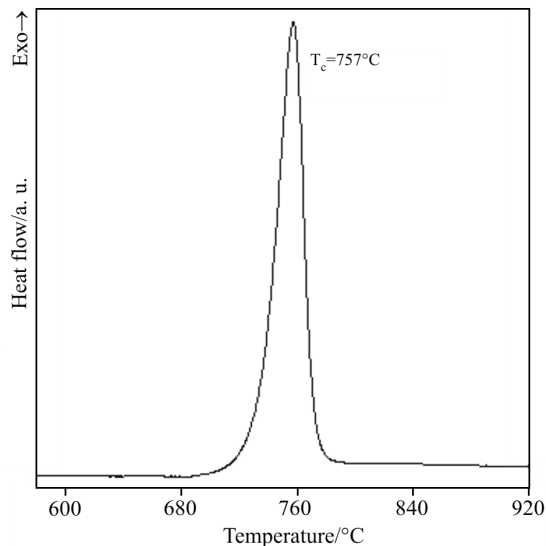


**Fig. 3** DSC curve for  $\text{SiO}_2\text{-Na}_2\text{O-CaO-P}_2\text{O}_5$  bioactive glass system (bulk) at heating rate of  $10^{\circ}\text{C min}^{-1}$  (heat flow)

lower temperature – becomes shorter and broader, resulting in an overlap of the second peak (higher temperature) with the first peak, after a critical value of powders' particle size (80–140  $\mu\text{m}$ ). Finally the DSC curve obtained from bulk bioactive glass system  $\text{SiO}_2\text{-Na}_2\text{O-CaO-P}_2\text{O}_5$ , (Fig. 3), presents one exothermic event at  $757^{\circ}\text{C}$  ( $T_c$ ) related to the formation of crystal phases, while the glass transition and the melting process are observed in temperature regions, where the respective characteristic processes of the powdered samples take place.

The presence of two crystallization peaks in the DSC curves of powdered samples can be attributed either to two distinct phase transformations or to two different crystallization mechanisms. In order to be exam-

ined the phases that are crystallized and the temperatures where they are crystallized, during the specific heat treatment, it is presented the FTIR study in powdered samples – with particle size  $<20\ \mu\text{m}$  – heated with the same heat treatment in three characteristic temperatures:  $900^{\circ}\text{C}$  – after the end of the temperature range of the two exothermic peaks –,  $700^{\circ}\text{C}$  – the temperature where the first crystallization peak arises – and  $570^{\circ}\text{C}$  – a temperature before the beginning of the range of the two exothermic peaks.

#### FTIR analysis

##### Samples heat treated up to $900^{\circ}\text{C}$

In a crystallized bioactive glass sample – in the system  $\text{SiO}_2\text{-CaO-Na}_2\text{O-P}_2\text{O}_5$  – heated at  $900^{\circ}\text{C}$  [9] there are two phases identified; sodium calcium silicate ( $\text{Na}_2\text{Ca}_2\text{Si}_3\text{O}_9$ ) being the major crystal phase present, and a second crystal phase that is calcium phosphate or an apatite-like phase ( $\text{Ca}_5(\text{PO}_4)_3\text{OH}$ ). All powdered samples heated with the same heat treatment up to  $900^{\circ}\text{C}$  present the same FTIR spectrum in agreement with the literature [9] for respective bioactive glass in the same system, heat treated under the same conditions. If these two phases were crystallized at different times e.g. different temperatures ranges, this would give rise to the two peaks in DTA trace. To be examined this possibility, there were studied by FTIR samples heated at  $700^{\circ}\text{C}$  – the lower temperature where the first crystallization peak ( $T_{cl}$ ) is present and before the end of temperature ranges of the two exothermic peaks.

##### Samples heat treated up to $700^{\circ}\text{C}$

In the FTIR spectra, (Fig. 4), peaks at wavenumbers 620,  $575\ \text{cm}^{-1}$  are commonly assigned to a calcium phosphate or apatite-like phase, as the dual peaks at about 575 and  $620\ \text{cm}^{-1}$  are attributed to P–O bending vibrations [10–12]. Additionally, there is a peak, at  $1040\ \text{cm}^{-1}$ , which can be attributed to the stretching  $\text{PO}_4$  vibration [13], although in the  $1000\text{--}1050\ \text{cm}^{-1}$  region the asymmetric vibration Si–O–Si is very strong resulting in the overlapping with the stretching  $\text{PO}_4$  vibrational peak.

From these results it is clear that the two phases are also detected at this temperature, suggesting the simultaneous growth of these phases. Consequently, the two crystallization peaks observed in the DSC curve of this sample – and of all powdered samples of this bioactive glass system – must not be due to a different phase development. In order to be excluded the possibility, one of these two phases to be crystallized at temperatures lower than the starting temperature of the first crystallization peak, bioactive glass samples

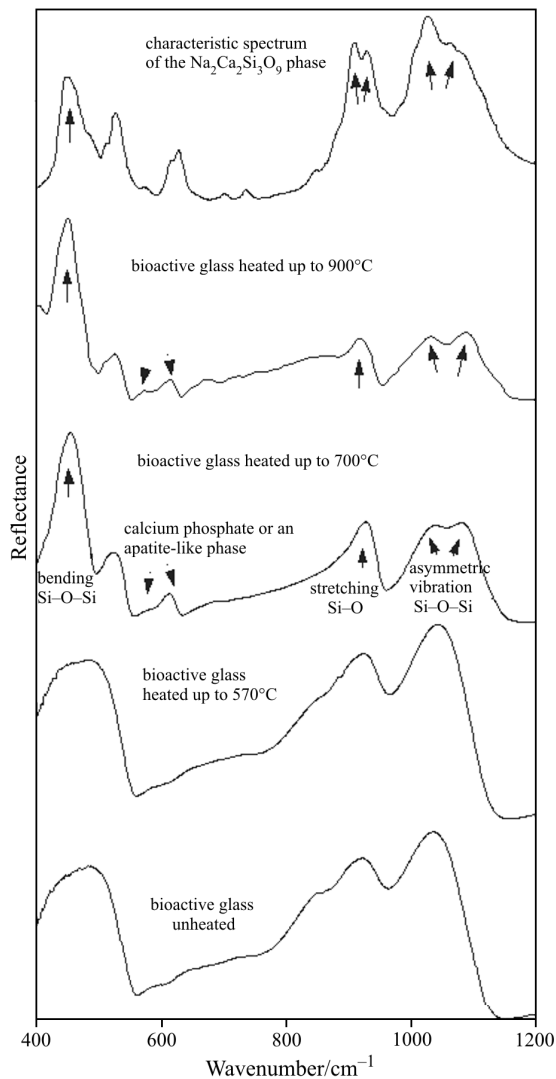


**Fig. 4** FTIR spectra of the  $\text{SiO}_2\text{-Na}_2\text{O-CaO-P}_2\text{O}_5$  bioactive glass system unheated, heated at 570, 700 and 900°C. Additionally is presented the characteristic spectra of the sodium calcium silicate ( $\text{Na}_2\text{Ca}_2\text{Si}_3\text{O}_9$ ) phase

with particle size  $<20\ \mu\text{m}$  were heated at 570°C, applying exactly the same heat treatment.

#### Samples heat treated up to 570°C

As it is observed from FTIR spectra, all the samples heated at temperatures lower than the starting temperature of the first crystallization peak, present the same characteristic peaks to those of unheated bioactive glass. This observation confirms the conclusion that the crystallization process of the two phases takes place simultaneously at the temperature range where the two exothermic peaks are detected.

XRD measurements on the same samples treated at respective temperatures (570, 700 and 900°C) supported the above conclusion [14].

As from the above studies it was concluded that the two crystallization peaks cannot be attributed to two distinct phase transformations, we examined the different crystallization mechanisms that occurred.

#### Study of exothermic peaks' parameters

Peak parameters in curves provide important information about nucleation and growth. Studies of the complete peak profile can often reveal features about the mode of crystallization and the evolving microstructure that are not manifested from the peak temperature. The DSC crystallization peak heights, ( $\delta T_c$ ), of nucleated glass as a function of the glass particle size, are shown in Fig. 5, while the crystallization peak temperature,  $T_c$ , increase with increasing particle size is presented in Fig. 6.

#### The dependence of $\delta T_c$ on particle size

It is clear from Fig. 5, that the crystallization height ( $\delta T_c$ ) of the second peak vs. particle size, remains almost unchanged. On the other hand,  $\delta T_c$  of the first crystallization peak decreases with increasing particle size.

The technique for identifying surface and bulk crystallization was developed by Ray and Day [15]. The dominant crystallization mechanism, surface or bulk, can be identified by determining the crystallization peak height ( $\delta T_c$ ) or the ratio  $T_c^2/\Delta T_c$  ( $\Delta T_c$  is the peak half width) as a decreasing or increasing function of the bioactive glass powder particle size. When the transformation proceeds only by internal nucleation and growth, the crystallization peak height ( $\delta T_c$ ) is pro-

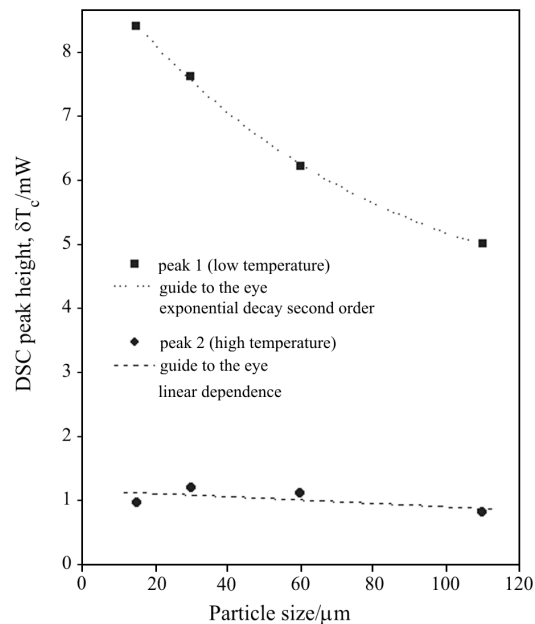


**Fig. 5** DSC crystallization peak height ( $\delta T_c$ ) for  $\text{SiO}_2\text{-Na}_2\text{O-CaO-P}_2\text{O}_5$  bioactive glass system at different particle sizes (heating rate  $10^\circ\text{C min}^{-1}$ )

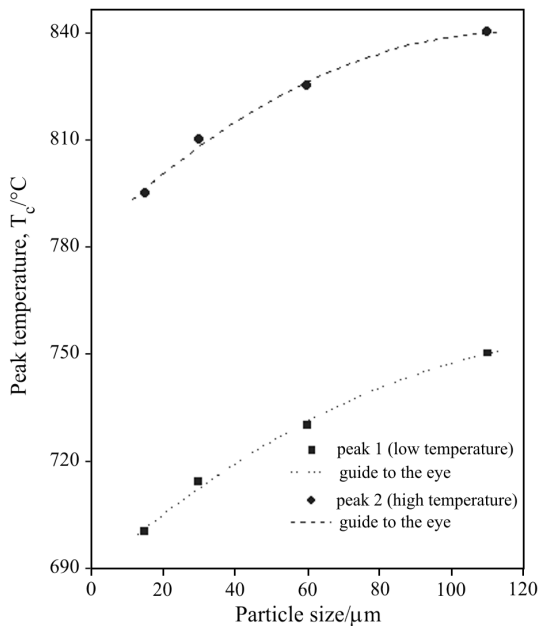


**Fig. 6** DSC crystallization peak temperature of  $\text{SiO}_2\text{-Na}_2\text{O-CaO-P}_2\text{O}_5$  bioactive glass system as a function of particle size (heating rate  $10^\circ\text{C min}^{-1}$ )

portional to the concentration of nuclei in the glass [16], and no change should be observed in  $\delta T_c$  as a function of particle size (for the same scan conditions and the same mass of sample). This behavior was observed in the second crystallization peak, indeed (Fig. 5). In reverse, the crystallization peak height ( $\delta T_c$ ) of the first peak decreases with increasing particle size. This behavior suggests that the particles crystallize primarily by surface crystallization, as in this case the peak height  $\delta T_c$  is proportional to the number of nuclei and simultaneously, the ratio of total surface area to volume, decreases with increasing particle size for the same total mass of sample. An ensemble of larger particles presents a considerably smaller surface area than an ensemble of smaller particles and thus, with the increase of particle size the number of surface nuclei is decreased. Therefore, the heat due to the surface crystallization is decreased with the increase of particle size, leading to the observed dependence. Consequently, the first crystallization peak is associated to surface nucleation and crystallization mechanisms while the second peak is associated to bulk nucleation and crystallization mechanisms.

#### The dependence of $T_c$ on particle size

As observed in Fig. 6, both crystallization peaks ( $T_c$ ) shift to lower temperatures. The maximum temperature  $T_{c1}$  (peak 1, low temperature) increases from 700 to  $750^\circ\text{C}$ , while the maximum temperature  $T_{c2}$  (peak 2, high temperature) increases from  $795$  to  $840^\circ\text{C}$  with increasing particle size. The behavior, shown in Fig. 6, is related to the particle size effects in

heat transfer. At a given heating rate, it is reasonable to suppose that larger particles present [17] higher heat transfer resistance, in comparison to small particles, so it takes longer for the center of the particle to reach the furnace temperature and therefore it is followed higher crystallization temperature.

The dependence of  $T_c$  on particle size, cannot readily provide information on the nature of the crystallization mechanism, i.e., whether it is a surface or an internal one. The shift in peak temperature as a function of particle size might present a simultaneous surface and volume crystallization. For small particles of powdered glasses, surface crystallization is the dominant mechanism, quickly transforming the particles. With the increase in the particle size the crystallization time – at a given temperature – increases due to the increasing importance of volume crystallization [18]. Also, it should be mentioned that even in the case that the particle size is less than  $20\ \mu\text{m}$ , this particle size is large enough to induce significant volume crystallization.

Finally, the peak half width,  $\Delta T_c$ , can also be used to predict whether a glass is transformed predominantly by surface or internal crystallization. Values of the ratio  $T_c^2/\Delta T_c$  can be calculated from the measured values  $T_c$  and  $\Delta T_c$ . The observed functional dependence of  $T_c^2/\Delta T_c$  on particle size, resembles closely that of  $\delta T_c$ .

#### Bioactive behavior vs. particle size

The differences in bioactive behavior of powdered samples as function of particle size, were followed through the process of immersion in SBF, of powder samples with different particle sizes and the same mass ( $m=40\ \text{mg}$ ), for one and two days. After the filtration, the characteristic transmittance spectra were received for each sample, in order to be examined the development of hydroxylcarbonate-apatite (HCAp) layer on the surface of the particles.

From the observed differences in the transmittance spectra of samples (Fig. 7, bold curves) can be followed a functional dependence of bioactive behavior on particle size.

Analytically, as presented in Fig. 7, the spectral regions where the most characteristic bands arise are  $1200\text{--}850$  and  $650\text{--}400\ \text{cm}^{-1}$  [19]. The main characteristics of the transmittance spectrum of the bioactive glass powder, before SBF, are attributed to the amorphous silica glass, e.g. the two bands at  $1040$  and  $920\ \text{cm}^{-1}$  assigned to Si–O–Si stretching vibration and a band at  $480\ \text{cm}^{-1}$  assigned to Si–O–Si bending one [20]. The formation of HCAp layer on the surface of the particles is recognized from the reduction and finally the disappearance of the silica glass bands and from evolution of the HCAp bands ( $1100\text{--}940$ ,  $600$ ,  $570\ \text{cm}^{-1}$ ) [21].

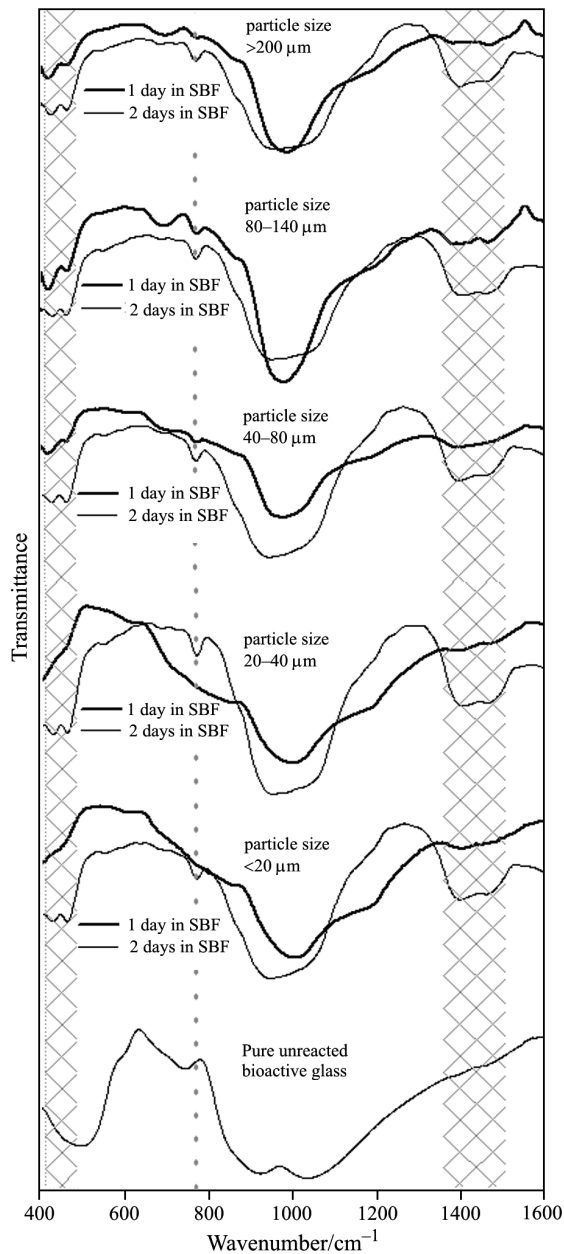


**Fig. 7** FTIR transmittance spectra of bioactive glass powder system  $\text{SiO}_2\text{-Na}_2\text{O-CaO-P}_2\text{O}_5$  with different particle sizes, after 1 day (bold curves) and two days (thin curves) in SBF

The spectra of the reacted powders, after 1 day in SBF, reveal new bands that can be assigned to a developed biological hydroxylapatite layer (HCAp) on particles' surface. Particularly, the strong band at  $\sim 1050\text{ cm}^{-1}$  is assigned to P-O stretching vibration and the two bands at  $610\text{-}600$  and  $560\text{-}550\text{ cm}^{-1}$  to P-O bending vibration of the developed HCAp layer [22–23]. Additional characteristic bands of HCAp layer are the weak at  $1530\text{-}1400\text{ cm}^{-1}$  assigned to C-O stretching vibration and one at  $878\text{ cm}^{-1}$  assigned to C-O out of plane bending vibration of carbonate group [24]. In Fig. 7 is observed that these

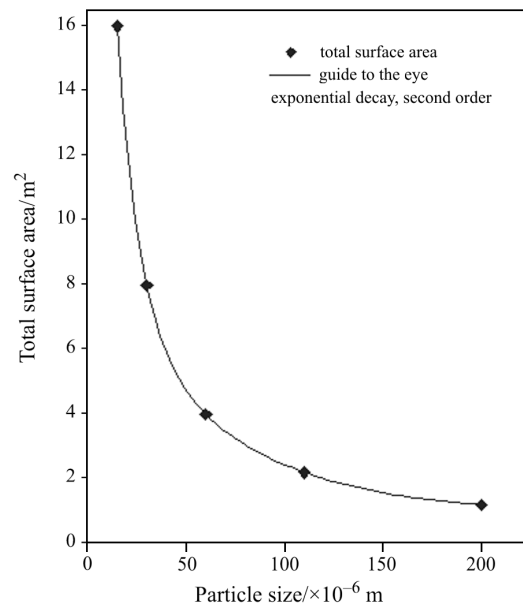


**Fig. 8** Total surface area dependence on particle size of powdered samples

characteristic bands become sharper and more definite, as the particle size of powders is increased until a specific size. From this observation is concluded that, increasing the particle size of powders up to  $80\text{ }\mu\text{m}$ , the bioactive response becomes better, while further increase in particle size does not lead in any further substantial improvement.

This behavior could be attributed to the dependence of total surface area, of each powdered sample, on the particle size which is illustrated in Fig. 8. The total surface area – for the same total mass of sample – decreases with increasing particle size, causing the decrease of the specific ratio of total surface area to volume of immersion liquid, since the volume of SBF is the same for all powdered samples. It is reported, that the decrease of the value of this specific ratio, induce a better bioactive response [25–27], however the value of this ratio does not present an important decrease for powders with particle size bigger than  $80\text{ }\mu\text{m}$  and consequently there is no further improvement of bioactive response of powders with particle size  $>80\text{ }\mu\text{m}$  and the reason is that the total surface area seem to decrease asymptotically with the increase of the particle size.

In the total surface calculation of each powdered sample it was considered that the geometry of each particle is spherical with a radius equal to the mean value of the particle range of each powdered sample.

For longer immersion time, all the samples – independently of their particle size – developed very good layer of hydroxylcarbonate-apatite. As it is presented in Fig. 7 (thin curves), the FTIR spectra of all samples after two days of immersion in SBF, confirm the formation of this HCAp layer on the surface of particles. Conse-

quently, with further than one day immersion, it is not observed any discrimination in the bioactive behavior.

## Conclusions

Thermal analysis measurements performed at specific heating rate on SiO<sub>2</sub>-Na<sub>2</sub>O-CaO-P<sub>2</sub>O<sub>5</sub> bioactive glass system in bulk and powder with different particle size forms were reported and discussed. Bulk glass gave one crystallization peak that was developed to two distinct exothermic crystallization peaks in powdered samples. These different peaks could not be attributed to the development of different phases. It was confirmed that the two crystallization peaks occurred due to different crystallization mechanisms. The height of the first DSC peak (at low temperature) was decreased with increasing particle size, thus indicating that the mechanism of surface crystallization could be associated with this peak. The height of the second DSC crystallization peak (at high temperature) remained unchanged with increasing particle size indicating a volume crystallization mechanism. The shift of the T<sub>c</sub> to lower temperatures, with the decrease of particle size, is related to the particle size effects on heat transfer. Additionally, a functional dependence of bioactive behavior on particle size was observed through the FTIR spectra of the immersed in SBF powdered samples. The bioactive response is improved with the increase of the particle size of powders up to 80 μm and then, remains almost unchanged with any further increase.

## Acknowledgements

It is acknowledged the support of the Greek Ministry of Education and European Community under the program Pythagoras II.

## References

- 1 X. Chatzistavrou, T. Zorba, K. Chrissafis, E. Pavlidou, E. Kontonasaki, P. Koidis and K. M. Paraskevopoulos, MEDICTA 2005: Proc. of the 7<sup>th</sup> Mediterranean Conference on Calorimetry and Thermal Analysis, Eds M. Lalia-Kantouri, Thessaloniki, Greece 2005, p. 200.
- 2 G. Rizzi, A. Scrivani, M. Fini and R. Giardino, *Int. J. Artif. Organs*, 27 (2004) 649.
- 3 X. Chatzistavrou, K. Chrissafis, E. Polychroniadis, E. Kontonasaki, P. Koidis and K. M. Paraskevopoulos, *J. Therm. Anal. Cal.*, in press  
DOI: 10.1007/s10973-005-7166-x.
- 4 G. C. Koumoulidis, C. C. Trapalis and T. C. Vaimakis, *J. Therm. Anal. Cal.*, 84 (2006) 165.
- 5 T. Ozawa, *Polymer*, 12 (1971) 150.
- 6 K. Matusita, S. Sakka and Y. Matsui, *J. Mater. Sci.*, 10 (1975) 961.
- 7 T. Kokubo, H. Kushitani, S. Sakka, T. Kitsugi and T. Yamamuro, *J. Biomed. Mater. Res.*, 24 (1990) 721.
- 8 S. B. Cho, K. Nakanishi, T. Kokubo, N. Soga, C. Ohtsuki, T. Nakamura, T. Kitsugi and T. Yamamuro, *J. Am. Ceram. Soc.*, 78 (1995) 1769.
- 9 X. Chatzistavrou, T. Zorba, E. Kontonasaki, K. Chrissafis, P. Koidis and K. M. Paraskevopoulos, *Phys. Status Solidi*, 201 (2004) 944.
- 10 C. Rey, M. H. Kim, L. Gerstenfeld and J. M. Glimcher, *Connect Tissue Res.*, 35 (1996) 343.
- 11 I. Rehman and W. Bonfield, *J. Mater. Sci.-Mater. Med.*, 8 (1997) 1.
- 12 M. H. Kim, C. Rey and J. M. Glimcher, *J. Bone Min. Res.*, 10 (1995) 1589.
- 13 A. Stoch, W. Jastrzebski, A. Brozek, B. Trybalska, M. Cichocinska and E. Szarawara, *J. Mol. Struct.*, 511/512 (1999) 287.
- 14 X. Chatzistavrou, N. Kantiranis, E. Kontonasaki, K. Chrissafis, P. Koidis and K. M. Paraskevopoulos, submitted (2006).
- 15 C. S. Ray and D. E. Day, *Thermochim. Acta*, 280/281 (1996) 163.
- 16 C. S. Ray and D. E. Day, *J. Am. Ceram. Soc.*, 73 (1990) 439.
- 17 W. Li and B. S. Mitchell, *J. Non-Cryst. Solids*, 255 (1999) 199.
- 18 C. S. Ray, D. E. Day, W. Huang, K. Lakshmi Narayan, T. S. Cull and K. F. Kelton, *J. Non-Cryst. Solids*, 204 (1996) 1.
- 19 M. R. Filgueiras, G. La Torre and L. L. Hench, *J. Biomed. Mater. Res.*, 27 (1993) 445.
- 20 G. Berger and M. Giehler, *Phys. Status Solidi*, 86 (1984) 532.
- 21 C. D. Clupper and L. L. Hench, *J. Mater. Sci.-Mater. Med.*, 12 (2001) 917.
- 22 M. Ogino, F. Ohuchi and L. L. Hench, *J. Biomed. Mater. Res.*, 14 (1980) 55.
- 23 F. Garcia, J. L. Arias, B. Mayor, J. Pou, I. Rehman, J. Knowles, S. Best, B. Leon, M. Perez-Amor and W. Bonfield, *J. Biomed. Mater. Res.*, 43 (1998) 69.
- 24 B. W. White, in 'The Infrared Spectra of Minerals', Edited by V. C. Farmer (Mineralogical Society, SW7 5HR, London 1974), p. 274.
- 25 M. Filgueiras, G. La Torre and L.L. Hench, *J. Biomed. Mater. Res.*, 27 (1993) 445.
- 26 Ö. Andersson, K. Vähätalo, R. Happonen, A. Yli-Urpo and K. Karlsson. In: Ö. Andersson, R. Happonen, A. Yli-Urpo, Eds Bioceramics Volume 7, Proceedings of the 7<sup>th</sup> International Symposium on Ceramics in Medicine. Turku, Finland: Butterworth-Heinemann Ltd., 1994, p. 67.
- 27 D. Greenspan, J. Zhong and G. La Torre, In: Ö. Andersson, R. Happonen, A. Yli-Urpo, Eds Bioceramics Volume 7, Proceedings of the 7<sup>th</sup> International Symposium on Ceramics in Medicine. Turku, Finland: Butterworth-Heinemann Ltd., 1994, p. 55.

Received: August 1, 2005

Accepted: May 5, 2006

DOI: 10.1007/s10973-005-7165-y